Synthesis of Organic Compounds in Planetary Nebulae and Proto-Planetary Nebulae

Sun Kwok

Department of Physics, Faculty of Science, University of Hong Kong
Hong Kong, China

Abstract. Recent millimeter-wave and infrared spectroscopic observations have found evidence of rapid synthesis of complex organic molecules in the late stages of stellar evolution. The chemical synthesis begins with the formation of acetylene, the first building block of benzene, in carbon stars. In the following proto-planetary nebulae stage, emission features corresponding to stretching and bending modes of aliphatic compounds are detected. When these objects evolve to become planetary nebulae, aromatic C-H and C-C stretching and bending modes become strong. These results show that complex carbonaceous compounds can be produced in a circumstellar environment over a period of only a few thousand years.

Isotopic analysis of meteorites and interplanetary dust collected in the upper atmospheres have revealed the presence of pre-solar grains similar to those formed in evolved stars. This provides a direct link between star dust and the solar system and raises the possibility that the early solar system was chemically enriched by stellar ejecta.

INTRODUCTION

The element carbon (C), which is the basic atom in the structure of organic compounds, is synthesized in asymptotic giant branch (AGB) stars through helium-burning (triple-α) reaction. The newly formed C atoms are then dredged up from the core to the surface of the star. Due to the low temperature of the photosphere of AGB stars, the C atoms can react with other atoms to form molecules such as carbon monoxide (CO). When the abundance of C overtakes that of oxygen (O), the surplus of C atoms after the formation of CO can be used to form other carbon-based molecules such as C_2, C_3, CN, etc. The spectral characteristics of these molecules in the photospheric spectra defines the class of AGB stars which we call carbon stars. Although we do not yet have a complete understanding of which AGB stars (e.g., within what mass range of progenitors) will evolve into carbon stars, we generally assume that they represent an evolved phase of AGB evolution.

In addition to its photospheric spectroscopic signature, carbon stars can also be identified through their circumstellar spectral properties. AGB stars undergo extensive mass loss through a stellar wind driven by radiation pressure on grains [1] and the mass loss rates of evolved O-rich or C-rich AGB stars can reach as high as 10^{-4} $M_\odot$ yr^{-1}. Chemical reactions in the stellar wind allow for the synthesis of other more complex gas-phase molecules, whose rotational transitions can be detected by millimeter-wave or submillimeter-wave spectroscopic observations. To date, more then 50 gas-phase molecules have been identified in the stellar winds of AGB stars. These molecules include inorganics (CO, SiO, SiS, NH_3, AlCl, etc), organics, (C_2H_2, CH_4, H_2CO, CH_3CN, etc.), radicals (CN, C_2H, C_3, HCO^+), rings (C_3H_2), and chains (HC_3N, HC_5N, etc.)[2].

Solid-state particles, both amorphous and crystalline, are also found to be condensing in the stellar winds of carbon stars. The most common solid-state condensate is amorphous silicates and silicon carbide (SiC), which lattice virbational modes at 10/18 μm and 11.3 μm are widely detected in O-rich and C-rich AGB stars respectively [3]. Since solid particles have a high opacity to visible light, the condensation in the circumstellar envelope can cause large obscuration to the light from the central star. The intercepted starlight heats up the dust particles, which

in turn cools by self radiating in the infrared. As the ejection rate increases in the late stages of AGB evolution, the envelope can contain so much dust that the star is completely obscured by dust extinction. Such stars will have no optical counterpart and can only be identified by infrared observations. An example of such infrared stars discovered in the *Infrared Astronomical Satellite (IRAS)* all-sky survey is IRAS 21318+5631 (Fig. 1). This carbon star has such a dense dust envelope that the central star suffers from 360 magnitudes of extinction in the visible (A_V), and is completely obscured [4]. Its infrared spectrum has a color temperature of 300 K and is the result of emission from a dust envelope heated by a hidden central star of 2500 K. The identification of these infrared objects as extremely evolved AGB stars and the spectroscopic observations of these objects have led to the realization that these stars are prolific molecular factories.
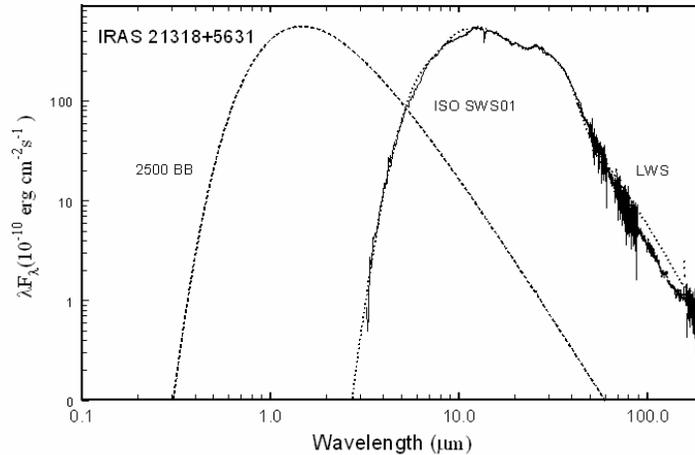

FIGURE 1. IRAS 21318+5631 is an example of an evolved carbon star so obscured by its own ejected circumstellar dust envelope that the central star is totally undetectable in the optical region. Its infrared spectrum (solid lines: *ISO SWS01 and ISO LWS*) is completely due to dust emission and has a color temperature of 300 K. The dotted line represents the theoretical fit to the spectrum based on a one-dimensional radiation transfer model with a hidden 2,500 K central star (dashed line) as the energy source. The absorption feature near the peak of the spectrum is the 1.37-μm band of acetylene, a molecule synthesized in the circumstellar envelope near the end of the AGB evolution.


BEYOND THE ASYMPTOTIC GIANT BRANCH

The high rate of mass loss on the AGB will eventually deplete the hydrogen envelope of the star and gradually expose the hot core. As the envelope thins to below 10^{-3} $M_\odot$, the star will begin to increase in temperature. Through a combination of H-shell burning and mass loss, the envelope becomes thinner, leading to an increase of stellar temperature. When the stellar temperature reaches 20,000 K, the ultraviolet photon output from the star will begin to photoionize the circumstellar envelope, creating a planetary nebula (PN, [5]). The intervening phase between the end of AGB and the onset of photoionization, is called the proto-planetary nebula (PPN) phase [6,7].

Although PNe are bright visible objects because of their emission-line spectrum, recent observations of PNe in the infrared and millimeter wavelengths have shown that they also possess thick molecular envelopes mixed with solid-state particles. Mid- and far-infrared observations from the *IRAS* and *Infrared Space Observatory (ISO)* missions have found that dust emission represents a major fraction of energy output from PNe (Fig. 2). The detection of molecular/dust envelopes in PNe clearly establishes the link to their progenitor AGB stars [8].

The existence of the remnant AGB dust envelope allows for the search of PPNe, as they are expected to have infrared colors intermediate between those of evolved AGB stars and young PNe [9]. The first PPNe (AFGL 618 and AFGL 2688) were discovered as the result of ground-based follow-up of the Air Force Geophysical Laboratory infrared sky survey. However, a comprehensive understanding of the PPN phenomenon was possible only after a systematic search for these objects among cool *IRAS* sources [6]. Although PPNe are faint in the visible due to the absence of emission lines, their structure can be observed through scattered light from circumstellar dust. The optical images of four PPNe obtained from observations with the *Hubble Space Telescope (HST)* are shown in Figure 3.
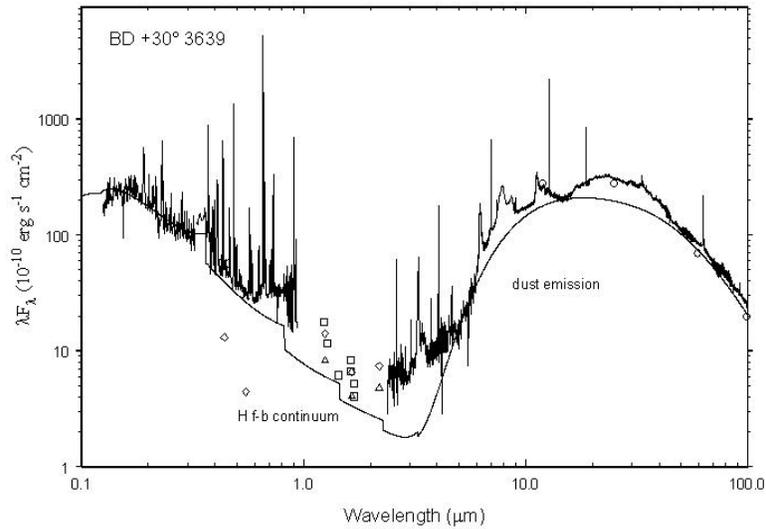
FIGURE 2. The spectral energy distribution of the PN BD+30 3639 showing the strong dust emission from the remnant of the AGB envelope. The spectrum of PNe is characterized by strong line emissions from the recombination lines of H and He and collisionally excited lines of metals in the UV, visible, and infrared regions. In the visible and near-IR, the continuum (approximated by the solid line) is due to nebular *b-f* emission, whereas beginning around $\lambda \sim 5$ μm, dust emission dominates the continuum. Some of the broad emission features in the IR are due the stretching and bending modes of aromatic compounds.
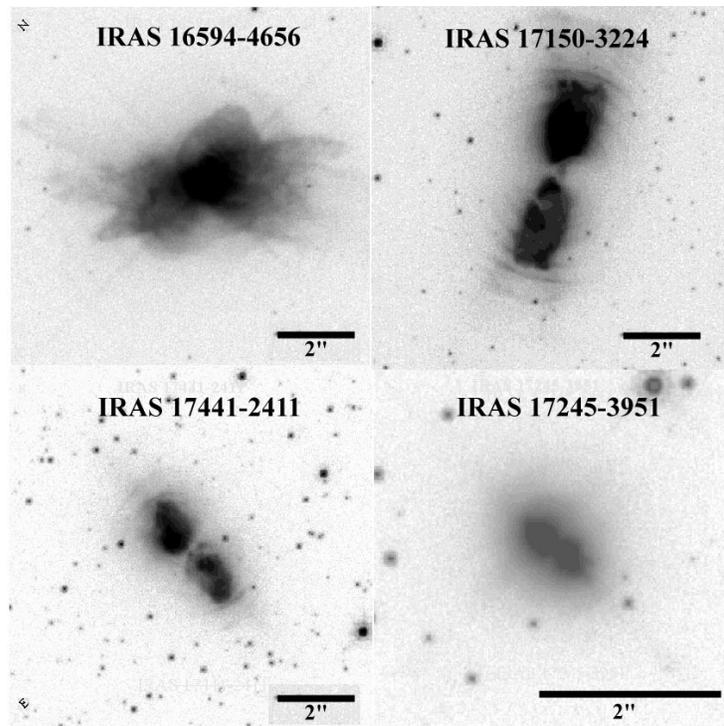

FIGURE 3. The *HST* images of four PPNe discovered in the ground-based follow-up of cool *IRAS* sources. Top left: the Waterlily Nebula [10], top right: the Cotton Candy Nebula [11], bottom left: the Silkworm Nebula [12], bottom right: the Walnut Nebula [10].

The approximately ten thousand years of evolution between the late AGB and the PN phase represent the most fascinating laboratory for astrochemistry. O-rich PPNe such as IRAS 17150-3224 and IRAS 17441-2411 (Fig. 3) show the same 10 and 18 μm emission features of amorphous silicates that are commonly seen in O-rich AGB stars. Carbon-rich PPNe (such as IRAS 16594-4656 and 17245-3951 in Fig. 3) show signatures of organic compounds of aromatic and aliphatic structures. Molecular and solid-state species of increasing complexity are being produced in the circumstellar environment. By the stage of PNe, crystalline silicates have begun to appear and organic compounds with aromatic structures are common. By observing the spectral changes of the envelope as a function of evolution, we are able to directly determine the chemical steps through which complex organic and inorganic compounds are made in space.

ORGANIC COMPOUNDS

A family of strong infrared emission features at 3.3, 6.2, 7.7, 8.6, 11.3 and 12.7 μm were first detected by the *Kuiper Airborne Observatory (KAO)* in the young C-rich PN NGC 7027 [13], and these features have since been widely observed in PNe, H II regions, reflection nebulae, and galaxies (Fig. 4). These features are identified with the aromatic C–H stretch (3.3 μm), aromatic C–C stretch (6.2 and 7.7 μm), aromatic C–H in-plane bend (8.6 μm), and aromatic C–H out-of-plane bending (11.3 μm) modes [14]. These features are collectively referred to as aromatic infrared bands (AIB).

The AIB features first make their appearance in the PPN phase. To this date, no AIB feature has been seen in AGB stars, suggesting that they are synthesized in the circumstellar envelope during the post-AGB phase. After the discovery of PPNe, ground-based and *ISO* observations have found that many C-rich PPN possess strong emission features at 3.4 and 6.9 μm, which are later identified as due to aliphatic C–H stretch and bending modes respectively [15, 16, 17]. Furthermore, emission features at 11.3, 12.1, 12.4, and 13.3 μm, which can be identified as arising from out-of-plane vibrational modes of aromatic C-H bonds with respectively 1, 2, 3, or 4 C–H bonds per edge of an aromatic ring, have also been detected [16].
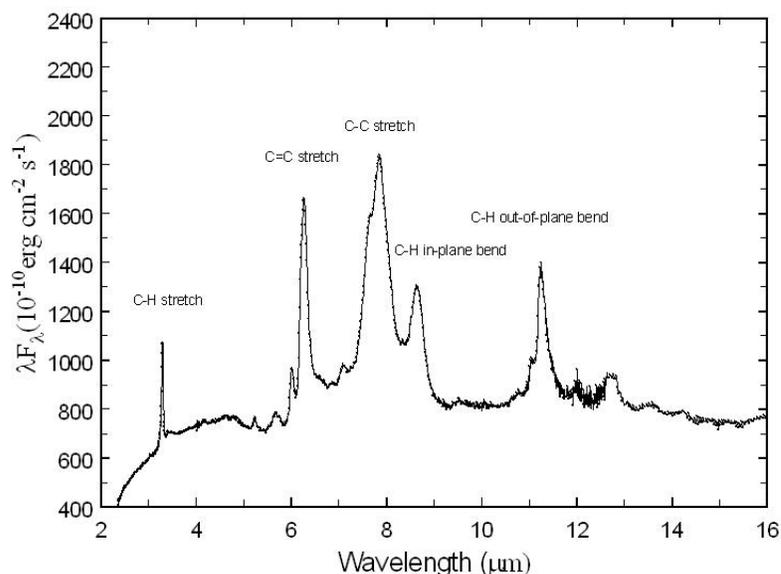
FIGURE 4. The *ISO SWS* spectrum of HD 44179 (the Red Rectangle) shows strong aromatic features on top of a continuum. Because of the low temperature of the central star (B8-A0), there is no atomic emission line in the spectrum.

Aromatic and aliphatic bands are not the only emission features seen in the infrared spectrum of PPNe. Also present are broad emission features at 8 and 12 μm. Since the 6.9-μm band is known to originate from a mixture of - –CH₂– and –CH₃ bending modes, associated bending modes of other side groups are quite likely to be present. Similarly, the 11.3-μm aromatic C–H out-of-plane bending mode can be accompanied by a complex set of features due to out-of-plane vibrations of alkenes [18]. The existence of the 8 and 12-μm broad emission features therefore suggests that the chemical structures of these carbonaceous compounds are complex, and probably include a variety of alkane and alkene side groups attached to aromatic rings.
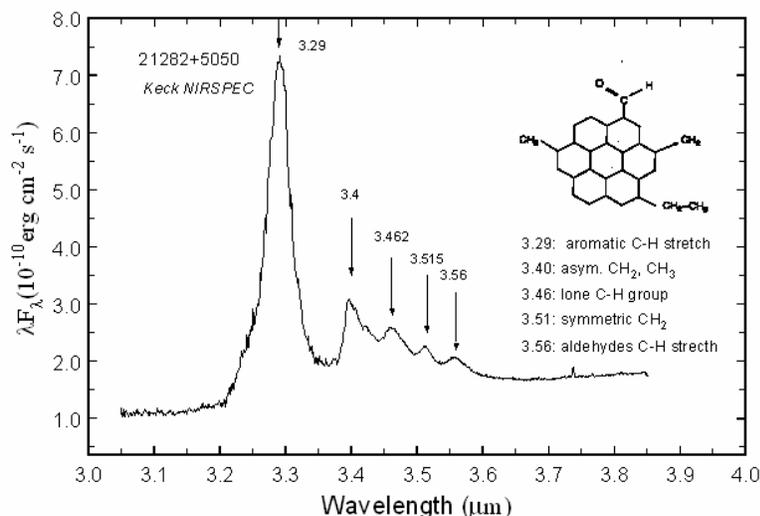
FIGURE 5. The spectrum of IRAS 21282+5050 taken with the NIRSPEC instrument at Keck Observatory showing the stretching modes of CH₂ and CH₃ sidegroups, as well as the 3.56 μm feature due to aldehydes [19].

## ORIGIN OF THE AROMATIC AND ALIPHATIC EMISSION FEATURES

The discovery of aromatic features has led to vigorous discussions in the literature on the nature of the carriers. Most of the suggestions center on aromatic hydrocarbons, both natural and artificially created substances. For example, carbonaceous nanoparticles have been produced by chemical vapor deposition [20], combustion [21], laser ablation [22], and laser pyrolysis of hydrocarbons [23]. Below we summarize some of the most popular models, and discuss their relevance in the circumstellar environment.

- Polycyclic Aromatic Hydrocarbons (PAH): PAH molecules are benzene rings of sp^2-hybridized C atoms linked to each other in a plane, with H atoms or other radicals saturating the outer bonds of peripheral C atoms. PAH molecules were first proposed as the carrier of the AIBs in the diffuse interstellar medium because their small sizes (<1 nm) allow them to be heated to high temperatures (~1000 K) by stochastic heating [24, 25, 26]. However, small gas-phase PAH molecules are unlikely to be the carrier of the AIB seen in PPNe and PNe. The AIBs in these objects always sit on top a strong continuum, which cannot be provided by small PAH molecules. The width of the AIB features and the consistency of the peak wavelengths also argue against the idea that they are produced by a mixture of different PAH molecules. The carrier is more likely to be a solid-state compound, consisting of at least hundreds of carbon atoms.

- Hydrogenated amorphous carbon: Hydrogenated amorphous carbon (HAC) consists of islands of aromatic (sp^2) bonded C atoms joined together with a variety of peripheral sp^2 and sp^3 bonded hydrocarbons [27]. HAC can be formed in the laboratory by direct condensation of carbon vapor from a H-rich atmosphere, and have been observed to show similar spectral features as in PPNe [28].
- Quenched carbonaceous composites (QCC): QCC are produced by the technique of hydrocarbon plasma deposition. Methane gas is heated to 3000 K with a microwave generator and allowed to expand into a vacuum chamber and condensed on a room-temperature substrate [29]. The resultant dark, granular material is shown by electron micrography to have an amorphous structure. Mass spectroscopy of QCC suggests that its aromatic component typically consists of 1 to 4 rings, and most have only 1-2 rings. Infrared spectroscopy of QCC reveals a mixture of $sp, sp^2,$ and sp^3 bonds. Since the conditions under which QCC is synthesized resemble the circumstellar environment of AGB stars, its laboratory production may shed some light on the solid-state condensation process in the envelopes of AGB and post-AGB stars [30].
- Kerogen: Coal, formed from fossilized hydrocarbon materials, also contains a mixture of $sp, sp^2,$ and sp^3 bonds like HAC and QCC. The possibility that coal-like material (e.g., kerogen) can be responsible for the AIB was first suggested by R. Papoular [31]. Structurally, kerogen can be represented by random arrays of aromatic carbon sites, aliphatic chains ($-CH_2-$)$_n$), and linear chains of benzenic rings with functional groups made up of H, O, N, and S attached. Comparison of the infrared spectra of kerogen shows that they are very similar to those of PPNe [32, 33, 34].

UNIDENTIFIED EMISSION FEATURES

In addition to the aromatic and aliphatic emission features, there are also a number of unidentified emission features in PPN and PN whose origin is not yet understood. Since they are mainly seen in C-rich stars, they are generally believed to originate from a carbonaceous compound.
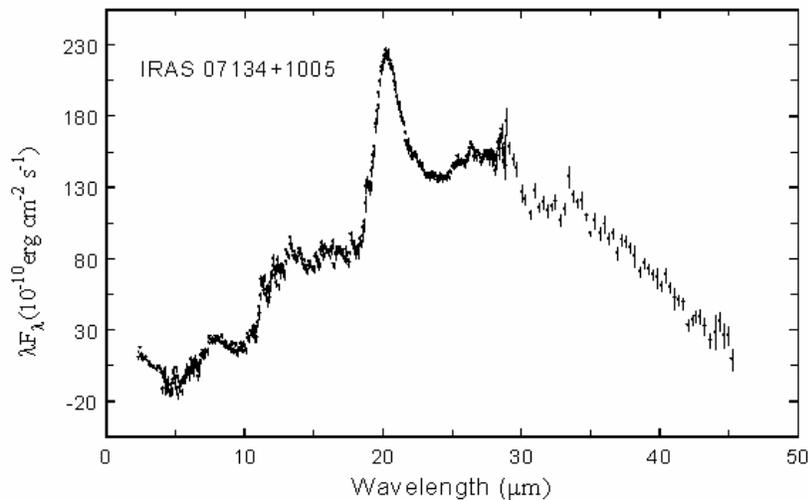
FIGURE 6. The *ISO SWS* spectrum of the PPN IRAS 07134+1005 showing the strong unidentified 21-µm emission feature.

The 21-µm Feature

The 21-µm feature was first discovered in four PPNe from observations by the *IRAS LRS* [35] (Fig. 6). High resolution ($\Delta\lambda/\lambda{\sim}2000$) *ISO* observations have found that all features have the same intrinsic profile and peak wavelength (20.1 µm) [36]. There is no evidence for any discrete sub-structure due to molecular bands in the

observed spectra, suggesting that the 21-μm feature is either due to a solid substance or a mixture of many similarly structured large molecules. There are 12 known 21-μm sources; all are C-rich stars in the post-AGB phase of evolution (e.g., the Water Lily Nebula in Fig. 3). This strongly suggests that the carrier of this feature is carbon-based. Possible candidates that have been proposed include large PAH clusters, HAC grains, hydrogenated fullerenes [37], nanodiamonds [38], and TiC nanoclusters [39]. However, none of the candidates provide a satisfactory fit to the astronomical spectrum.

The 30-μm Feature

The emission feature around 30 μm was discovered in the spectra of carbon stars and PNe from *KAO* observations [40]. More recently, the 30-μm feature is found to be common in C-rich PPNe, especially those showing the 21-μm emission feature [41]. The fact that a significant fraction (~20%) of the total luminosity of the object is emitted in this feature suggests that the carrier must be composed of abundant elements [42]. The first suggested identification was solid MgS based on a comparison with laboratory measurements [43]. The alternative suggestion that the carrier is a carbonaceous material continues to be popular because the feature is only seen in C-rich objects.
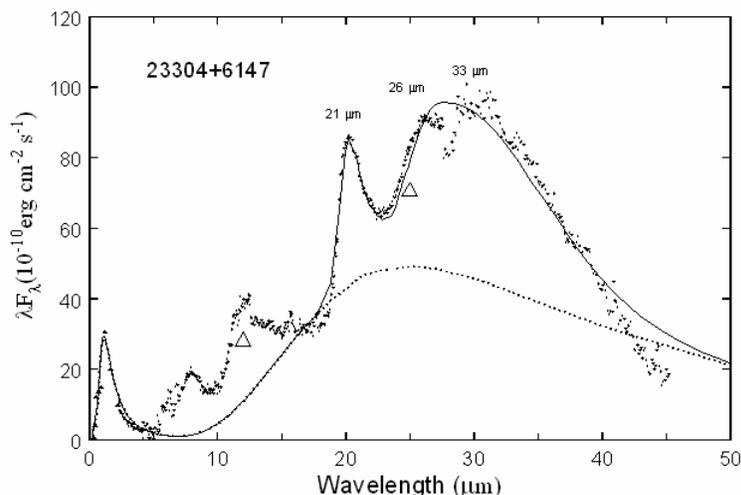
FIGURE 7. The *ISO SWS* spectrum of the PPN IRAS 23304+6147 shows strong 21- and 30-μm emission features. The dotted line is a fit to the continuum (assumed to be amorphous carbon) and the solid line is a radiative transfer fit to the spectrum including the 21- and 30-μm features but not the AIB features (from [44]).

Extended Red Emission

Extended red emission (ERE) is a broad ($\Delta\lambda \sim 80$ nm), featureless emission band with a peak wavelength between 650 and 800 nm. ERE was first detected in the spectrum of HD44179 (the Red Rectangle, [45] and is commonly seen in reflection nebulae [46, 47]. ERE has also been detected in dark nebulae, cirrus clouds, planetary nebulae, HII regions, diffuse interstellar medium, and in haloes of galaxies [48].

Since many solids emit visible luminescence when exposed to UV light, it is assumed that ERE is a photoluminescence process powered by far UV photons. The wide presence of ERE in the diffuse ISM suggests that the carrier of ERE must be a major component of the ISM. This limits the chemical composition of the ERE carrier to a few abundant and highly depleted elements, such as C, Fe, Si, and Mg. Since metals do not undergo photoluminescence, the remaining possibilities are C and Si with carbonaceous materials being the most likely candidates.

Proposed carriers of the ERE include HAC [49. 46], QCC [50], C_{60} [51], and silicon nanoparticles [52, 53]. Diamond is a possible carrier for the ERE band [54]. The material is chemically robust, optically transparent, and capable of emitting luminescence from point defects. Recent laboratory studies of nanodiamonds with nitrogen-vacancy defect centers show luminescence closely resembles spectral profiles of the astronomical ERE [55]. Since nanodiamonds have the highest abundance (14000 ppm) among all presolar grains in meteorites, nanodiamonds are probably widely present in the interstellar medium and therefore satisfy the high abundance requirement for the carrier of ERE.

CHEMICAL EVOLUTION

The detection of organic compounds in the ejecta of evolved stars gives us important information on how these species are formed. The evolution from AGB to PPN to PN is very short, and this gives us the precise knowledge on the time scale of chemical synthesis. Since the AIB features first emerge in the PPN phase, what are the steps leading to the formation of ring molecules? Acetylene (C_2H_2), believed to be the first building block of benzene, is commonly detected in evolved carbon stars through its v_5 fundamental band at 13.7 μm (Fig. 8). Polymerization of C_2H_2 leads to the formation of diacetylene (C_4H_2) and triacetylene (C_6H_2) in PPN (Fig. 9), cumulating in the formation of benzene[56].
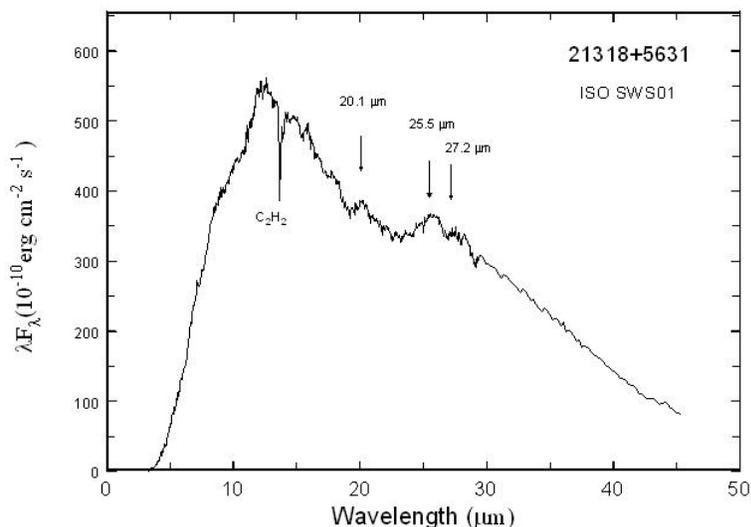
FIGURE 8. *ISO SWS01* spectrum of the carbon stars IRAS 21318+5631. The strong absorption feature at 13.7 is due to the v5 vibrational band of acetylene. The 21 and 30 μm features have also made their appearance in emission.

A summary of the change in the relative strengths of the infrared emission features as stars evolve from AGB to PNe is given in Table 1. The weakening of the 3.4 and 6.9 μm from PPNe to PNe suggests a change from aliphatic to aromatic structures. This could be the result of photochemistry where the onset of UV radiation modify the aliphatic side groups through isomerizations, bond migrations, cyclization and ring closures and transform them into ring systems [18]. Hydrogen loss can also result in fully aromatic rings that are more stable than alkanes or alkenes. Evidence for such H loss can also be found in the weakening of the 12.1, 12.4, and 13.3-μm features and the strengthening of the 11.3-μm feature from PPNe to PNe [17].
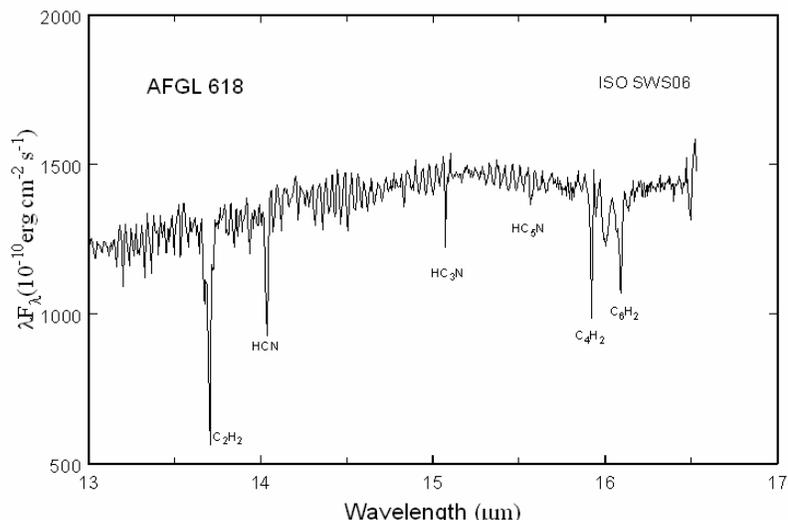
FIGURE 9. *ISO SWS06* spectrum of the PPN AFGL 618 showing absorption features of acetylene, diacetylene, and triacetylene as well as cyanopolyynes.

In comparison to interstellar clouds, there are many advantages of using circumstellar envelopes to study the process of chemical synthesis. First, there is only one single energy source – the central star, which temperature and luminosity are well known. The envelope often has a well-defined symmetry, making the geometry of the system simple. By using molecular lines and infrared continuum radiation as probes, the physical conditions of the envelope such as density, temperature, and radiation background *(ρ(r), T(r), I(r),* respectively) are well determined. Most importantly, the chemical reaction times are constrained by the dynamical and stellar evolution times, which are $\sim 10^4$ yr for AGB stars, 10^3 yr for PPNe, and 10^4 yr for PNe. These time scales give us a precise knowledge of the chemical time needed to form one species from another and therefore rigorously constrain the chemical models.

TABLE 1. Changes in relative strengths of IR emission features from AGB to PN

Emission features (μm)	Origin	Carbon Stars	PPN	PN
3.3, 6.2, 7.7, 8.6, 11.3	Aromatic stretch and bending modes	No	Yes	Strong
3.4, 6.9	C-H aliphatic stretch and bend	No	Yes	Weak
12.1, 12.4, 13.3	C-H out-of-plane bend with 2, 3, and 4 adjacent H atoms	No	Yes	Weak
Broad 8, 12	Bending modes from aliphatic sidegroups	No	Yes	Weak
Broad 21	-	Weak	Strong	No
Broad 30	-	Yes	Yes	No
ERE (0.6-0.8)	Carbonaceous nanoparticles (?)	No	Yes	Yes

STARDUST IN THE SOLAR SYSTEM

Spectral signatures of grains produced in AGB stars, PPNe, and PNe are now found in solar system objects. The silicate features, both amorphous and crystalline, are seen in comets and interplanetary dust [57]. Infrared spectra of organic extract sublimate from the Murchison meteorite show the 3.4-μm aliphatic features that are similar to those observed in PPNe [58]. This feature has also been observed in comets [59] and interplanetary dust [60]. Isotopic studies of meteorites have also identified grains of presolar origin, including diamonds [61], SiC [62], corundum and spinel [63]. These grains therefore represent an important link between stars and the solar system [64]. The dominant organic matter in carbonaceous chondrites is similar to kerogen. These results suggest that comets, interplanetary dust, and meteorites preserve pristine stellar material not processed by the early solar nebula, and our

ability to perform laboratory analysis of these materials through mass spectroscopic and isotopic analysis has given us a direct link to inorganic and organic compounds produced by stars.

CONCLUSIONS

We have learned that chemical synthesis of complex organic and inorganic compounds can take place in the low-density circumstellar environment over very short (10^3 yr) time scales during the late stages of stellar evolution. By tracing the change in the infrared spectra of carbon stars to PPNe to PNe, we found definite evidence for chemical evolution. Infrared spectroscopic observations have clearly demonstrated that solid-state compounds of both organic and inorganic nature are produced in abundance in the circumstellar envelopes of evolved stars. The ejection of these grains into the interstellar medium suggests that circumstellar grains is a major source of interstellar grains, some of which may have survived the formation of the solar system. The detections of pre-solar grains in meteorites and the detection of high deuterium to hydrogen ratio in interplanetary dust particles [65] have supported this stellar-solar system connection. The study of circumstellar chemistry therefore could have serious implications on our understanding of the origin of the solar system.

ACKNOWLEDGMENTS

REFERENCES

1. S. Kwok, *Astrophys. J.* **198**, 583-591 (1975)
2. H. Olofsson, *IAU Symp. 178*: *Molecules in Astrophysics: Probes and Processes*, edited by E. van Dishoeck (Kluwer, Dordrecht), 1997, pp. 457-468.
3. S. Kwok, K. Volk, and W.P. Bidelman, *Astrophys. J. Suppl.* **112**, 557-584 (1997).
4. K. Volk, G.-Z. Xiong, and S. Kwok, *Astrophys. J.* **530**, 408-417 (2000)
5. S. Kwok, *The Origin and Evolution of Planetary Nebulae*, Cambridge University Press (2000)
6. S. Kwok, *Ann. Rev. Astr. Ap.* **31**, 63-92 (1993)
7. H. Van Winckel, *Ann. Rev. Astr. Ap.* **41,** 391-427 (2003).
8. S. Kwok, *Astrophys. J.* **258**, 280-288 (1982).
9. S. Kwok, *Mon. Not. Roy. Astr. Soc.* **244**, 179-183 (1990)
10. B.J. Hrivnak, S. Kwok, and K.Y-L. Su, *Astrophys. J.* **524,** 849-856 (1999)
11. Kwok, S., Su, K.Y.-L., and B.J. Hrinvnak,, *Astrophys. J.* **501**, L117-L121 (1998)
12. Su, K.Y.-L., Volk, K., S. Kwok, and B.J. Hrivnak, *Astrophys. J.* **508**, 744-751 (1998)
13. R.W. Russell, B.T. Soifer, B.T. and S.P. Willner, *Astrophys. J.* **217**, L149-153 (1977).
14. W.W. Duley, and D.A. Williams, *Mon. Not. Roy. Astr. Soc.* **196**, 269-274 (1981).
15. T.R. Geballe, A.G.G.M. Tielens, S. Kwok, and B.J. Hrivnak, *Astrophys. J.* **387**, L89-91 (1992).
16. Kwok, S., Volk, K. & Hrivnak, B.J. *Astron. Astrophys.* **350**, L35-L38 (1999).
17. B.J. Hrivnak, K. Volk, and S. Kwok, *Astrophys. J.* **535**, 275-292 (2000).
18. S. Kwok, K. Volk, K., and P. Bernath *Astrophys. J.* **554**, L87-L90 (2001).
19. B.J. Hrivnak, S. Kwok, and T.R. Geballe, in preparation
20. A. Sakata, S. Wada, T. Onaka, and A.T. Tokunaga, *Astrophys. J.* **320**, L63-L67 (1987).
21. L. Colangeli, V. Mennella, P. Palumbo, A. Rotundi, and E. Bussoletti, *Astron. Astrophys. Suppl.* **113**, 561-577 (1995)
22. A. Scott, and W. W. Duely, *Astrophys. J.* **472**, L123-L125 (1996).
23. N. Herlin, I. Bohn, C. Reynaud, M. Cauchetier, A. Galvez, and J-N.Rouzaud, *Astron. Astrophys.* **330**, 1127-1135 (1998).
24. J.L. Puget, and A. Léger, A. *Ann. Rev. Astr. Ap.* **27**, 161-198 (1989).
25. L.J. Allamandola, A. G. G. M. Tielens, and J. R. Barker, *Astrophys. J.* Suppl. **71**, 733-775 (1989).
26. K. Sellgren, *Spec. Acta Part A.* **57**, 627-642 (2001).
27. A.P. Jones, W. W. Duley, and D. A. Williams, *Q. J. R. Astron. Soc.* **31**, 567-582 (1990)
28. A.D. Scott, W. W. Duley, and H. R. Jahani, *Astrophys. J.* **490**, L175-177 (1997).
29. A. Sakata, A. Wada, T. Tanabe, and T. Onaka, *Astrophys. J.* **287**, L51-L54 (1984).
30. S. Wada, and A. T. Tokunaga, A.T. in *Natural Fullerenes and Related Structures of Elemental Carbon*, edited by F.J.M. Rietmeijer, Springer, pp. 31-52 (2006)
31. R. Papoular, J. Conard, M. Giuliano, J. Kister, J., and G. Mille, *Astr. Ap.* **217**, 204-208 (1989).
32. O. Guillois, I. Nenner, R. Papoular, and C. Reynaud, *Astrophys. J.* **464**, 810-817 (1996).

33. R. Papoular, J. Conard, O. Guillois, I. Nenner, C. Reynaud, and J.-N. Rouzaud, *Astr. Ap.* **315**, 222-236 (1996).
34. R. Papoular, R. *Astr. Ap.* **378**, 597-607 (2001).
35. S. Kwok, K. Volk, and B.J. Hrivnak, *Astrophys. J.* **345**, L51-L54 (1989).
36. K. Volk, S. Kwok, and B. J. Hrivnak, *Astrophys. J.* **516**, l99-L102 (1999).
37. A. Webster, *Mon. Not. Roy. Astr. Soc.* **277**, 1555-1566 (1995).
38. H. G. M. Hill, A. P. Jones, and L. B. d'Hendecourt, *Astr. Ap.* **336**, L41-L44 (1998).
39. G. von Helden, A. G. G. M. Tielens, D. van Heijnsbergen, M. A. Duncan, S. Hony, L. B. F. M. Waters, and G. Meijer, *Science* **288,** 313-316 (2000).
40. W. J. Forrest, J. R. Houck, and J. F. McCarthy, *Astrophys. J.* **248** 195-200 (1981).
41. A. Omont, A. *et al., Astrophys. J.* **454**, 819-825 (1995).
42. B. J. Hrivnak, K. Volk, and S. Kwok, *Astrophys. J.* **535,** 275-292 (2000).
43. J. H. Goebel, and S. H. Moseley, *Astrophys. J.* **290**, L35-L39 (1985).
44. K. Volk, S. Kwok, B. J. Hrivnak, and R. Szczerba, *Astrophys. J.* **567**, 412-422 (2002)
45. G. D. Schmidt, M. Cohen, B. Margon, *Astrophys. J.* **239**, L133-138 (1980)
46. A. N. Witt, and R. E. Schild, *Astrophys. J.*, **325**, 837-845 (1988)
47. A. N. Witt, and T. D. Boroson, *Astrophys. J.*, **355**, 182-189 (1990)
48. T.L. Smith, and A. N. Witt, *Astrophys. J.* **565**, 304- (2002)
49. W. W. Duley, and D. A. Williams, *Mon. Not. Roy. Astr. Soc.*, **230**, 1P-4P (1988)
50. A. Sakata, S. Wada, T. Narisawa, Y. Asano, Y. Iijima, T. Onaka, and T. A. Tokunaga, *Astrophys. J.* **393**, L83-L86 (1992)
51. A. Webster, *Mon. Not. Roy. Astr. Soc*, **264**, L1 (1993)
52. A. N. Witt, K. D. Gordon, and D. G. Furton, *Astrophys. J.* **501**, L111-L115 (1998)
53. G. Ledoux, M. Ehbrecht, O. Guillois, F. Huisken, B. Kohn, et al., *Astr. Ap.* **333**, L39-L42 (1998)
54. W. W. Duley, *Astrophys. Sp. Sc.* **150**, 387-390 (1988)
55. H.-C. Chang, K. Chen, and S. Kwok, *Astrophys. J.* **639**, L63-66 (2006)
56. J. Cernicharo, A. M. Heras, A. G. G. M. Tielens, J. R. Pardo, F. Herpin, M. Guélin, and L. B. F. M. Waters, *Astrophys. J.* **546**, L123-L126 (2001).
57. S. Sandford, and R. M. Walker, *Astrophys. J.* **291**, 838-851 (1985).
58. Y. J. Pendleton, and L. J. Allamandola, *Astrophys. J. Suppl.* **138**, 75-98 (2002).
59. J. K. Davies, P. J. Puxley, M. J. Mumma, D. C. Reuter, S. Hoban, H. A. Weaver, and S. L. Lumsden, *Mon. Not. Roy. Astr. Soc.* **265**, 1022-1026 (1993).
60. S. J. Clemett, and C. R. Maechling, *Science* **262**, 721-725 (1993).
61. R. S. Lewis, T. Ming, J. F. Wacker, E. Anders, and E. Steel, *Nature* **326** 160-162 (1987).
62. T. Bernatowicz, G. Fraundorf, T. Ming, E. Anders, B. Wopenka, E. Zinner, and P. Fraundorf, *Nature* **330**, 728-730 (1987).
63. L. R. Nittler, C. M. O'D. Alexander, X. Gzo, R. M. Walker, and E. Zinner, *Astrophys. J.* **483**, 475-495 (1997).
64. E. Zinner, *Ann. Rev. Earth Planet. Sci.* **26**, 147-188 (1998).
65. S. Messenger, *Nature* **404**, 968-971 (2000).